

LETTERS

Magnetic impurity formation in quantum point contacts

Tomaž Rejec¹ & Yigal Meir^{1,2}

A quantum point contact (QPC) is a narrow constriction between two wider electron reservoirs, and is the standard building block of sub-micrometre devices such as quantum dots and qubits (the proposed basic elements of quantum computers). The conductance through a QPC changes as a function of its width in integer steps of $G_0 = 2e^2/h$ (where e is the charge on an electron, and h is Planck's constant), signalling the quantization of its transverse modes^{1,2}. But measurements of these conductance steps also reveal an additional shoulder at a value around $0.7G_0$ (refs 1–4), an observation that has remained a puzzle for more than a decade. It has recently been suggested^{5,6} that this phenomenon can be explained by the existence of a magnetic ‘impurity’ in the QPC at low electron densities. Here we present extensive numerical density-functional calculations that reveal the formation of an electronic state with a spin-1/2 magnetic moment in the channel under very general conditions. In addition, we show that such an impurity will also form at large magnetic fields, for a specific value of the field, and sometimes even at the opening of the second transverse mode in the QPC. Beyond explaining the source of the ‘0.7 anomaly’, these results may have far-reaching implications for spin-filling of electronic states in quantum dots and for the dephasing of quantum information stored in semiconductor qubits.

A QPC is usually formed by applying a negative voltage to a split gate (Fig. 1a), depleting the electrons in the two-dimensional electron gas (2DEG) under it to form a narrow and short constriction connecting large, two-dimensional regions of 2DEG. The number of occupied quantized transverse modes can be changed as a function of the applied gate voltage. As each mode contributes G_0 to the conductance (owing to spin degeneracy), the conductance rises in steps quantized at integer multiples of G_0 (refs 1, 2). A magnetic field lifts the spin degeneracy, leading to steps in multiples of e^2/h . Surprisingly, many experiments observe, at zero magnetic field, an additional shoulder near $0.7G_0$, a feature usually referred to as the 0.7 anomaly^{3,4}, which merges smoothly with the $0.5G_0$ plateau in a large magnetic field. Although less robust, an analogous anomaly was observed in the transition to the second conductance plateau at about $1.7G_0$ (ref. 4). A similar conductance structure was also found at large magnetic fields near crossings of spin-up and spin-down modes of different sub-bands⁷.

There have been several attempts to explain the 0.7 anomaly in terms of an antiferromagnetic Wigner crystal⁸, spontaneous sub-band splitting^{9–11}, or by assuming that the QPC supports a local quasi-bound state⁶. In the last case, as one electron is transported through this state, Coulomb interactions suppress the transport of an electron with opposite spin, reducing the conductance to around $0.5G_0$. The Kondo effect—the screening of this local spin by the conduction electrons—enhances the conductance at low temperatures towards G_0 . Indeed, experiments⁵ reveal features characteristic of the Kondo effect and the continuous evolution of the conductance

from $0.7G_0$ at higher temperatures to G_0 at low temperatures. But how can a QPC, being an open system, support a quasi-bound state? Previous numerical investigations report conflicting results^{12–14}. Below we present detailed spin-density-functional theory¹⁵ (SDFT) calculations showing that such a local moment can indeed form as the conductance of a QPC rises towards the first plateau. Additionally we present evidence that the formation of a quasi-bound state may also lead to the observed 1.7 anomaly and the anomaly at the crossing of sub-bands in large magnetic fields.

The set-up we used in our calculation is shown in Fig. 1b. In order to make the calculation tractable, we modelled the reservoirs as semi-infinite quantum wires. They are wide enough to carry many modes and thus resemble well the two-dimensional reservoirs in experimental set-ups. Using SDFT within the local spin-density approximation, we calculated the spin densities of the 2DEG and the charge distribution on the electrodes self-consistently. The nonlinearity of the equations may lead to several stable solutions that differ in their energy (details of our numerical approach are given in the Methods section). Here we present results for a specific QPC, as described in Fig. 2. However, the results are generic: we studied QPCs of lithographic length from 100 nm to 400 nm, of lithographic width from

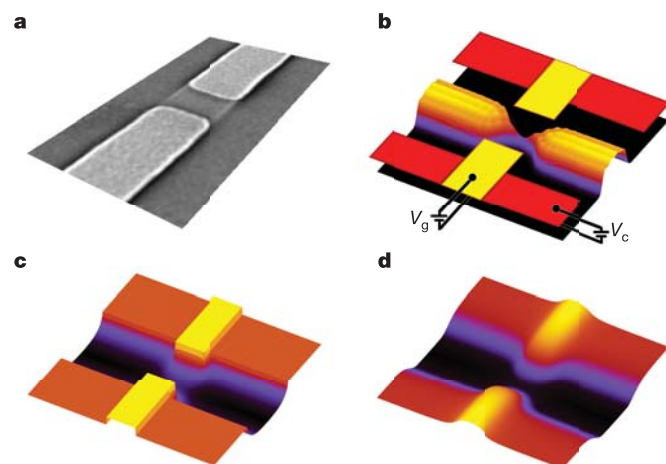


Figure 1 | Quantum point contact. **a**, Micrograph of a split gate forming a QPC. (Image from ref. 5, with permission.) **b**, The set-up used in the calculation. Voltage (V_g) applied to split gates (yellow) forms a QPC between two quantum wires defined by negatively biased (V_c) confining electrodes (red). Also shown is the density of the 2DEG near pinch-off where only one mode is occupied within the QPC, while the quantum wires carry several modes. The colour scale extends from zero (black) to $0.85 \times 10^{11} \text{ cm}^{-2}$ (yellow). **c**, **d**, Typical potentials in the plane of the electrodes (**c**) and in the 2DEG (**d**). Potentials on the electrodes are constant and are the input to the calculation, determining the effective potential in the plane of the 2DEG.

¹Department of Physics, ²The Ilse Katz Center for Meso- and Nano-Scale Science and Technology, Ben Gurion University, Beer Sheva 84105, Israel.

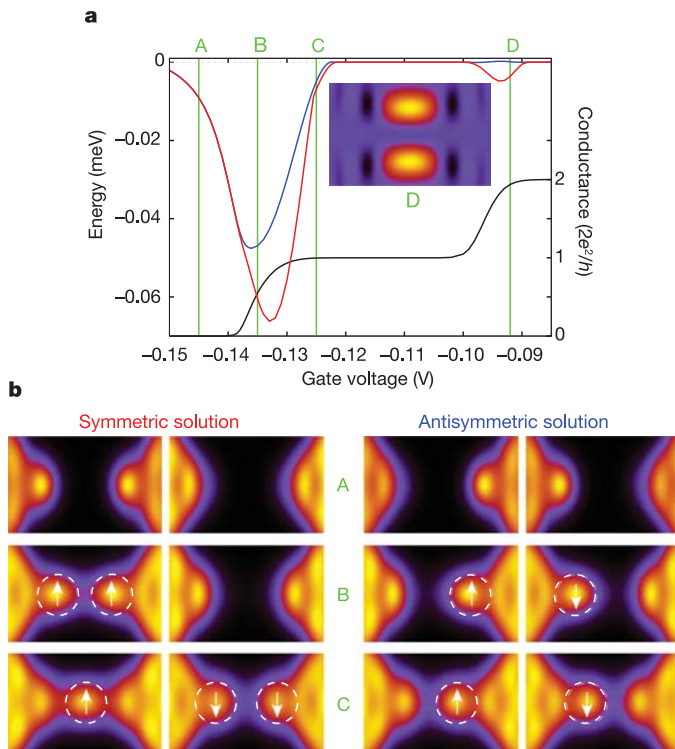


Figure 2 | States with spin polarization in a QPC. The QPC with a lithographic width and length of 200 nm and 250 nm, respectively, forms a constriction in a quantum wire with a lithographic width of 300 nm. The confining electrodes are biased to $V_c = -0.08$ V. The donor layer provides an electron density of 10^{11} cm^{-2} , and is 20 nm below the surface. The 2DEG forms 50 nm below the surface. **a**, Energies of the symmetric (red) and antisymmetric (blue) spin-polarized solutions relative to the energy of the unpolarized solution. Polarized solutions appear in the transition from pinch-off to the first plateau and then on the rise to the second plateau. The black line is a rough approximation to the conductance of the QPC, as calculated from the Kohn-Sham wavefunctions of the unpolarized solution (right-hand scale). Note, however, that for the lowest-energy, polarized solution the first conductance plateau will start around $V_g = -0.122$ V, on the right of point C. **b**, Spin densities of the symmetric and antisymmetric solutions for spin-up electrons (left columns) and spin-down electrons (right columns) at three values of gate voltage as indicated in **a**. The colour scale extends from zero (black) to $0.35 \times 10^{11} \text{ cm}^{-2}$ (yellow). A 400-nm-long and 100-nm-wide region about the centre of the QPC is shown. At A, the QPC is pinched-off; there are two polarized regions on each side of the QPC. At B, the two polarized regions begin to overlap. At C, in the symmetric solution the electrons in the QPC rearrange in such a way that a spin-1/2 magnetic moment forms. The inset to **a** shows spin polarization in the symmetric solution just below the second conductance plateau, at point D.

150 nm to 250 nm, and with 2DEG electron densities from 10^{11} to $2 \times 10^{11} \text{ cm}^{-2}$, with very similar results.

We first consider a QPC in the absence of a magnetic field. For gate voltages corresponding to conductance plateaus there is a unique solution to our equations, which shows no spin polarization. Although such a solution is also present in the regions between the plateaus, additional solutions exhibiting spin polarization in the QPC appear there. We classify these solutions according to their spatial symmetry: in the 'symmetric' and 'antisymmetric' solutions the polarization is respectively the same or opposite on the two sides of the QPC. In Fig. 2a, the energies of the polarized solutions relative to the energy of the unpolarized solution are plotted for gate voltages from pinch-off to the second conductance plateau. The symmetric solution, when present, is always the ground state of the system.

Figure 2b shows the evolution of spin densities of the two polarized solutions from pinch-off to the point where a spin-1/2 magnetic moment forms in the QPC. At point A the QPC is pinched-off: there

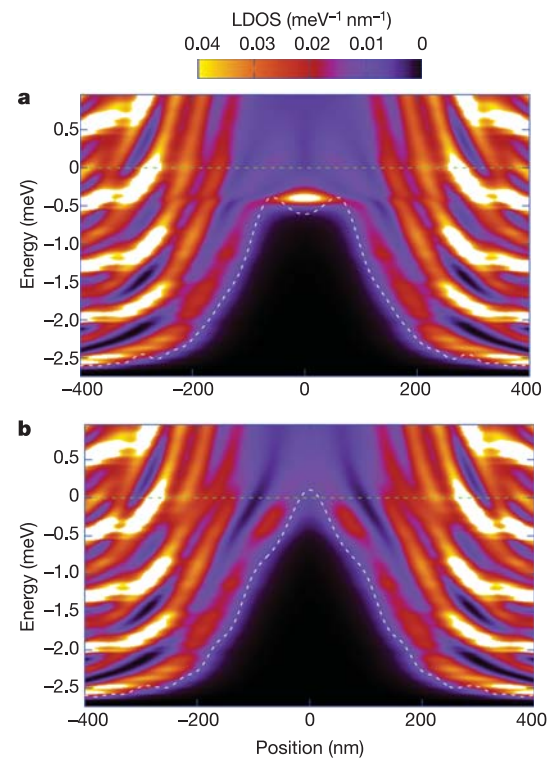


Figure 3 | Formation of a magnetic moment. **a**, Spin-up and **b**, spin-down local densities of states (LDOS), integrated over the cross-section of the QPC, for the QPC from Fig. 2 at $V_g = -0.125$ V. The Kohn-Sham potential for electrons in the lowest transverse mode is also shown (white dashed line). The potential for spin-up electrons has a double-barrier form near the centre of the QPC, and supports a quasi-bound state about 0.5 meV below the Fermi energy (green dashed line). Spin-down electrons also form quasi-bound states in the shoulders of the potential on both sides of the QPC. The bright stripes on both sides of the QPC correspond to the quasi-one-dimensional bands of the reservoirs.

is an extended region about the centre of the QPC where the density vanishes as the potential is much higher than the Fermi energy. The potential decreases towards the reservoirs and at some point it crosses the Fermi energy. Here are regions where the electron gas is polarized: the density is very low and the gain in (negative) exchange energy outweighs the additional kinetic energy incurred by polarization. The two polarized regions on both sides of the QPC do not overlap in this regime. The degeneracy of the ground state is thus fourfold: each of the polarized regions is spin-degenerate. With increasing gate voltage, the potential at the QPC gets lower and the electron density drifts inwards, forming narrow fingers that eventually reach the centre of the QPC (point B in Fig. 2). In the process, the polarized regions become increasingly decoupled from the reservoirs: two quasi-bound states, each corresponding to roughly one electron, form on each side of the QPC. As the potential barrier at the centre of the QPC gets weaker, the tunnelling probability through the barrier becomes appreciable and the conductance increases from zero. On increasing the gate voltage even further, a different configuration becomes energetically favourable in the symmetric subspace: a single electron forms a weakly coupled quasi-bound state at the centre of the QPC, accompanied by two electrons of opposite spin in regions further away towards the reservoirs (point C in Fig. 2). The degeneracy of the ground state is now twofold: the QPC acts as a spin-1/2 magnetic impurity. The spin-resolved local density of states (LDOS), that is, the number of states per energy and length interval (Fig. 3), provides additional insight into this state. The QPC potential for one of the spin components assumes a double-barrier form (due to Friedel oscillations), and a resonant state forms in its minimum.

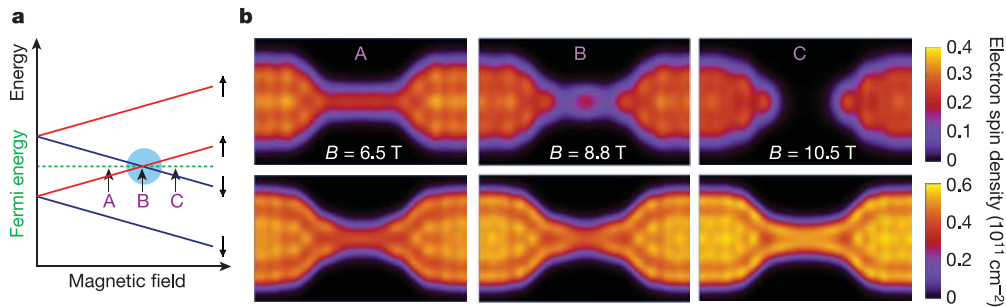


Figure 4 | Quasi-bound state in a large magnetic field. **a**, The Zeeman splitting of mode energies at the top of a QPC. The energy of the spin-up electrons in the lowest mode crosses the energy of the spin-down electrons in the higher mode at some value of the magnetic field. At a specific value of the gate voltage this crossing occurs near the Fermi energy. **b**, Spin-up (top row) and spin-down (bottom row) electron densities at three values of a magnetic field B near the degeneracy point. A 800-nm-long and 250-nm-wide area is

shown. At $B = 6.5$ T (point A in **a**), one mode is open for both spin orientations. At $B = 10.5$ T (point C), there are two open modes for spin-down electrons and none for spin-up electrons. In between, the bands cross and a quasi-bound state forms in the QPC ($B = 8.8$ T, point B). The QPC parameters are as in Fig. 2 except for the lithographic length, which is 300 nm. The gate voltage is $V_g = -0.102$ V.

The length of the QPC affects the formation of the spin-1/2 magnetic moment. In very short contacts, the transition to a well defined quasi-bound state does not take place at all: as the two polarized regions merge at the centre of the QPC, the conductance has already reached the first plateau. For longer contacts, the transition to the magnetic moment state shifts towards the pinch-off. In very long contacts, the configuration in Fig. 2b (symmetric solution at point C) evolves into an antiferromagnetically ordered chain.

The situation is somewhat similar on the rise from the first to the second conductance plateau: the density of electrons in the second mode is low there, and exchange again stabilizes states with a polarized QPC (Fig. 2a inset). This mechanism is not as efficient here as it was in the first mode: polarization in the second mode also induces (owing to exchange) partial polarization in the first mode. As the density in the first mode is large, there is a high kinetic energy cost involved. This is consistent with the experimental observation that not all QPCs exhibit the 1.7 anomaly.

In an external in-plane magnetic field, the energies of transverse modes for the two spin components split. The resulting polarized non-degenerate solution does not generally support a quasi-bound state. However, as shown in Fig. 4a, at a particular value of the field the energy of spin-up electrons (those with spin parallel to the field) in the first mode crosses that of spin-down electrons in the second mode. By tuning the gate voltage, one can also make the energy of the degeneracy point coincide with the Fermi energy. Figure 4b shows the evolution of spin densities with magnetic field in the vicinity of this crossing. At the degeneracy point a well-defined quasi-bound state forms, but, unlike the zero-field solution, it has a definite spin, determined by the field. This may be the source of the ‘0.7 analogues’ observed at high magnetic fields⁷.

The formation of a local spin-degenerate quasi-bound state (supported by the extensive SDFT calculations presented here) is a necessary condition for the Kondo effect, which is beyond the local spin-density approximation used here. Interestingly, the calculations indicate that near pinch-off, two such states form on the two sides of the QPC. This may lead to the physics of the two-impurity Kondo model. Depending on the ratio of the coupling between these impurities, and their couplings to their respective reservoirs, one would expect to observe a zero-bias anomaly, with a split zero-bias peak, in this regime^{16,17}. The splitting should increase with increasing conductance. The formation of such polarized states at the QPC may also affect the spin-filling of quantum dots formed between two QPCs. Additionally, as quantum dots have been proposed as qubits (the building blocks of quantum computers), these degenerate quasi-bound states must be considered seriously—the degeneracy allows decoherence of quantum processes at very low temperatures. As short decoherence times will degrade the performance of any quantum computer, it will be necessary to ensure that the QPCs

forming the qubits are outside the quasi-bound-state formation regime.

METHODS

Model. We treated the 2DEG, electrodes and the donor layer as a set of three electrostatically coupled strictly two-dimensional systems. We assumed the donor layer was uniform and fully ionized. Then, according to spin-density-functional theory¹⁸, the properties of the system can be uniquely determined in terms of spin densities $n_{\uparrow}(\mathbf{r})$ and $n_{\downarrow}(\mathbf{r})$ of the 2DEG and by the distribution of charge on the electrodes $n_{el}(\mathbf{r})$ (\mathbf{r} is the position in either the plane of the 2DEG or the plane of the electrodes). In particular, the energy of the system is a functional of the densities:

$$E[n_{\uparrow}, n_{\downarrow}, n_{el}] = E_{es}[n_{\uparrow}, n_{\downarrow}, n_{el}] + T_s[n_{\uparrow}, n_{\downarrow}] + E_{xc}[n_{\uparrow}, n_{\downarrow}] + \frac{1}{2}g\mu_B \int d\mathbf{r} B(\mathbf{r}) [n_{\uparrow}(\mathbf{r}) - n_{\downarrow}(\mathbf{r})] - \sum_i N_i V_i$$

Here $E_{es}[n_{\uparrow}, n_{\downarrow}, n_{el}]$ is the electrostatic energy of the charge distribution. The presence of the semiconductor was taken into account through the use of the GaAs dielectric constant $\kappa = 12.9$ and a modified form of the Coulomb interaction, reflecting the dielectric mismatch at the surface¹⁹. We treated the 2DEG quantum-mechanically by including its kinetic energy (T_s) and exchange-correlation energy (E_{xc}) in the energy functional, taking into account that the effective mass of electrons in GaAs is 0.067 times the bare electron mass. We used the local spin-density approximation for the exchange-correlation functional, as parameterized in ref. 20. The fourth term in the energy functional is the Zeeman energy due to an in-plane magnetic field, with $g = 1.9$ for GaAs quantum wires⁷. Finally, as we compared the energies of different solutions at fixed voltages between electrodes and the 2DEG, we applied a Legendre transform to the energy functional (the last term in the expression above), with N_i and V_i being respectively the number of electrons and the voltage on i th electrode, and the sum running over all the electrodes in the system. The correct densities minimize the above functional subject to the applied voltages, and a constraint that the total number of electrons should match the charge provided by the donor layer.

Calculations. The minimization procedure yields Kohn-Sham equations¹⁵ for the 2DEG, with a constant electrostatic potential on each of the electrodes. In each iteration of the self-consistency loop, we first solved for the Kohn-Sham scattering states and calculated the density of the 2DEG. Using an iterative approach, we then redistributed the remaining electrons on electrodes in such a way that the potential there assumed the required form. In this step we performed the calculation on a large rectangular box, with periodic boundary conditions, which enabled us to employ the fast Fourier transform method and thus make the calculation efficient. We used the resulting charge distribution to calculate an improved electrostatic potential in the 2DEG. To obtain spin-polarized solutions at zero external magnetic field, we broke the symmetry by applying a magnetic field of an appropriate form (spatially symmetric or antisymmetric) in the initial iterations of the self-consistent procedure.

Received 10 April; accepted 5 July 2006.

- van Wees, B. J. *et al.* Quantized conductance of point contacts in a two-dimensional electron gas. *Phys. Rev. Lett.* **60**, 848–850 (1988).

2. Wharam, D. A. *et al.* One-dimensional transport and the quantisation of the ballistic resistance. *J. Phys. C* **21**, L209–L214 (1988).
3. Thomas, K. J. *et al.* Possible spin polarisation in a one-dimensional electron gas. *Phys. Rev. Lett.* **77**, 135–138 (1996).
4. Thomas, K. J. *et al.* Interaction effects in a one-dimensional constriction. *Phys. Rev. B* **58**, 4846–4852 (1998).
5. Cronenwett, S. M. *et al.* Low-temperature fate of the 0.7 structure in a point contact: A Kondo-like correlated state in an open system. *Phys. Rev. Lett.* **88**, 226805 (2002).
6. Meir, Y., Hirose, K. & Wingreen, N. S. Kondo model for the “0.7 anomaly” in transport through a quantum point contact. *Phys. Rev. Lett.* **89**, 196802 (2002).
7. Graham, A. C. *et al.* Interaction effects at crossings of spin-polarised one-dimensional subbands. *Phys. Rev. Lett.* **91**, 136404 (2003).
8. Matveev, K. A. Conductance of a quantum wire in the Wigner-crystal regime. *Phys. Rev. Lett.* **92**, 106801 (2004).
9. Kristensen, A. *et al.* Bias and temperature dependence of the 0.7 conductance anomaly in quantum point contacts. *Phys. Rev. B* **62**, 10950–10957 (2000).
10. Reilly, D. J. Phenomenological model for the 0.7 conductance feature in quantum wires. *Phys. Rev. B* **72**, 033309 (2005).
11. DiCarlo, L. *et al.* Shot-noise signatures of 0.7 structure and spin in a quantum point contact. *Phys. Rev. Lett.* **97**, 036810 (2006).
12. Berggren, K.-F. & Yakimenko, I. I. Effects of exchange and electron correlation on conductance and nanomagnetism in ballistic semiconductor quantum point contacts. *Phys. Rev. B* **66**, 085323 (2002).
13. Starikov, A. A., Yakimenko, I. I. & Berggren, K.-F. Scenario for the 0.7-conductance anomaly in quantum point contacts. *Phys. Rev. B* **67**, 235319 (2003).
14. Hirose, K., Meir, Y. & Wingreen, N. S. Local moment formation in quantum point contacts. *Phys. Rev. Lett.* **90**, 026804 (2003).
15. Kohn, W. & Sham, L. J. Self-consistent equations including exchange and correlation effects. *Phys. Rev.* **140**, A1133–A1138 (1965).
16. Georges, A. & Meir, Y. Electronic correlations in transport through coupled quantum dots. *Phys. Rev. Lett.* **82**, 3508–3511 (1999).
17. Aguado, R. & Langreth, D. C. Out-of-equilibrium Kondo effect in double quantum dots. *Phys. Rev. Lett.* **85**, 1946–1949 (2000).
18. Hohenberg, P. & Kohn, W. Inhomogeneous electron gas. *Phys. Rev.* **136**, B864–B871 (1964).
19. Jackson, J. D. *Classical Electrodynamics* 2nd edn 147 (Wiley, New York, 1975).
20. Tanatar, B. & Ceperley, D. M. Ground state of the two-dimensional electron gas. *Phys. Rev. B* **39**, 5005–5016 (1989).

Acknowledgements We thank N. Argaman, R. Baer, D. Goldhaber-Gordon, B. I. Halperin, K. Kikoin, W. Kohn and M. Stopa for discussions. This work was supported by the Binational Science Foundation. We also thank the Department of Theoretical Physics at Jožef Stefan Institute for providing access to computer facilities.

Author Contributions Y.M. initiated the project. T.R. performed numerical simulations. T.R. and Y.M. analysed results and co-wrote the paper.

Author Information Reprints and permissions information is available at www.nature.com/reprints. The authors declare no competing financial interests. Correspondence and requests for materials should be addressed to T.R. (tomaz.rejec@ijs.si).